Structure and dynamics of water inside endohedrally functionalized carbon nanotubes

Sanjib Paul, T. G. Abi, and Srabani Taraphder

Citation: The Journal of Chemical Physics **140**, 184511 (2014); doi: 10.1063/1.4873695
View online: http://dx.doi.org/10.1063/1.4873695
View Table of Contents: http://scitation.aip.org/content/aip/journal/jcp/140/18?ver=pdfcov
Published by the AIP Publishing

Structure and dynamics of water inside endohedrally functionalized carbon nanotubes

Sanjib Paul,[1] T. G. Abi,[2] and Srabani Taraphder[1]
[1]*Department of Chemistry, Indian Institute of Technology, Kharagpur 721302, India*
[2]*Department of Chemistry, Sacred Heart College Thevara, Kochi 682013, India*

(Received 7 January 2014; accepted 17 April 2014; published online 14 May 2014)

We have carried out classical molecular dynamics simulations on the formation of extended water chains inside single-walled carbon nanotubes (SWCNTs) in water in the presence of selected functional groups covalently attached to the inner wall of the tube. Analogues of polar amino acid sidechains have been chosen to carry out the endohedral functionalization of SWCNTs. Our results show a spontaneous and asymmetric filling of the nanotube with dynamical water chains in all the cases studied. The presence of Asp- and Glu-like sidechains is found to result in the formation of well-ordered water chains across the tube having the maximum number of water molecules being retained within the core with the largest residence times. The presence of methyl or methylene groups along the suspended chain is observed to disrupt the formation of water chains with higher length and/or longer residence times. The importance of hydrogen bonding in forming these water chains is assessed in terms of the relaxations of different hydrogen bond correlation functions. For a given dimension of the hydrophobic nanopore, we thus obtain a scale comparing the ability of carboxylic, alcohol, and imidazole groups in controlling the structure and dynamics of water in it. Our results also suggest that SWCNTs of varying lengths, endohedrally functionalized with Asp- and Glu-like sidechains, may be used as design templates in CNT-based water storage devices. © *2014 AIP Publishing LLC*. [http://dx.doi.org/10.1063/1.4873695]

I. INTRODUCTION

Hydrophobic interactions are known to be critical in determining unique functions of biological channels facilitating the transport of ions and water across the cell membrane.[1] Narrow water-filled pores have also been suggested as building blocks for high selectivity/high-flux membranes for molecular devices in fuel cells.[2] In general, the presence of suitable functional group(s) such as polar amino acid residues at key positions along the channel results in the desired specificity of interactions and high levels of selectivity required by its unique biological function. These functional groups may also increase the lifetime of one or more water molecules within the nanopore. Retention of water, if possible, within a channel-like environment for a long time may be used in building a template for water storage devices. It is thus important to understand, for example, how the structure and dynamics of water molecules are governed by the presence of certain polar amino acid residues in a hydrophobic confinement. In view of their relatively simple structures and dimensions comparable to typical ion channels,[2,3] single-walled carbon nanotubes (SWCNT) have been extensively used in literature as the prototype of hydrophobic nanopores.[4–9] The aim of the present article is to investigate the properties of confined water using classical molecular dynamics studies in *functionalized* SWCNTs having sidechain analogues of polar amino acid residues covalently attached to the CNT wall and suspended inside the hydrophobic core.

When placed in water, SWCNTs, in spite of their hydrophobic nature, are continuously and spontaneously filled with a one dimensionally ordered chain of water molecules, as reported from molecular dynamics simulation studies.[8,10] The driving force behind this seemingly counter-intuitive observation has been investigated in detail to understand the competing contributions of entropy and enthalpy changes associated with the transfer of water from bulk to the hydrophobic interior of the narrow SWCNTs. Initial studies, involving explicit calculation of the grand canonical partition function for confined water, reported a near-zero entropy of transfer from bulk into a quasi-infinite nanotube.[11] On the other hand, a positive transfer of entropy was predicted using the density of states formalism.[12] In this study, the formation of only two hydrogen bonds by each water molecule along the confined water chain is shown to lead to a considerable gain in entropy that compensates for the apparent energetic and entropic penalties associated with the transfer of water molecules from the bulk polar environment to a hydrophobic interior of the channel.[12] Most recently, based on their extensive molecular dynamics simulation studies on (6, 6) SWCNT in TIP3P water, Waghe *et al.*[13] estimated the entropy of transfer of water from bulk to be about $-1.3\ k_B$ per molecule (k_B: Boltzmann constant) and spontaneous filling of SWCNTs was found to be driven by a favorable decrease in energy.[13]

The motion of water molecules inside CNTs exhibits several interesting features. Rotational relaxation of water molecules inside the hydrophobic core shows bistability following an angular jump mechanism to go from one stable state to another, crossing a free energy barrier of about $2.5\ k_BT$.[14] Hydrogen bonding, a unique feature underlying several bulk water properties, is also found to contribute importantly to water structure and dynamics inside SWCNTs.

The intermittent hydrogen bond time correlation function, $C(t)$ has been shown to decay very slowly inside CNT compared to bulk water[15] with the rate of decay decreasing with a decrease in the nanotube diameter. Hydrogen bond lifetime between internal water molecules, calculated from the continuous hydrogen bond time correlation function, $S(t)$, shows an interesting variation with the diameter of the tube. Compared to bulk water, these lifetimes are found to be much longer in (6, 6) CNTs and markedly shorter inside (8, 8), (10, 10), (12, 12), and (20, 20) CNTs. The unique dynamical behaviour of water inside SWCNTs in turn facilitates transport of molecules and ions through them. For instance, transfer of an excess proton mediated by the water chain through carbon nanotubes is found to be 40 times faster than that in bulk water[16] with the rate of proton transfer increasing with an increase in the tube length.[17] Interestingly, *ab initio* and QM-MM molecular simulations studies reveal that a hydroxide ($-OH^-$) ion moves faster than a hydronium ion (H_3O^+) inside (6, 6) CNT in sharp contrast to their mobilities in bulk water.[17]

Functionalized carbon nanotubes (FCNTs) are now indispensable in the designing of novel CNT-based materials with better solubility and biocompatibility.[18–24] FCNTs have also been extensively used in theoretical and simulation studies to model the nature of flow of liquid inside the nanotube. Molecular dynamics studies on ionic flow in CNTs functionalized at the two open ends with $-COOH$ groups amply demonstrate how selectivity between cation and anion permeation may be achieved.[25] The presence of a carboxylic group attached to the inner wall alters the hydrophobicity of the inner cavity and was found to allow faster permeation of a mixture of water and methanol in a continuous flow instead of a pulsed behaviour.[26] Gong *et al.*[27] presented a theoretically designed molecular sieve by embedding a (9, 9) SWCNT vertically between two graphite sheets and endohedrally attaching eight or 16 carbonyl groups to mimic the structure of potassium channel in membrane spanning proteins. Molecular dynamics studies of Na^+ and K^+ ion transport through these channels demonstrated remarkable dependence of ion channel selectivity on the functionalization pattern of the carbonyl group.[27]

It is evident from the above discussion that appropriate functionalization of the hydrophobic nanopore may be useful in attaining the desired control over the properties of FCNTs. In the present work, we shall focus on endohedral functionalization using analogues of polar amino acid residues that are widely known to play crucial roles in several biological channels. For example, in human aquaporin 5 (HsAQP5), orientation of His173 regulates the pore radius of selectivity filter (SF) between the *narrow* and *wide* states.[28] His67, in this system, is key to blocking the cytoplasmic end (CE) of the channel thus enabling the latter to alter between the *closed* and *open* states.[28] Proton transfer from the entry channel (CP) to the exit channel (EC) via the retinal-Schiff base is known to involve Asp side chains located on both sides of the retinal Schiff base (CP and EC) in bacteriorhodopsin.[29] Proton translocation in D-channel of heme-copper oxidases (HCOX) to binuclear heme-copper site is also known to occur through Glu242.[29] In the present work, we have chosen to work with FCNTs endohedrally functionalized with analogues of polar amino acid sidechains such as His, Asp, Glu, Thr, and Ser. Needless to say, our models are highly idealized and do not even attempt to capture the complexity associated with any of the systems mentioned above. Instead, our specific goal here is to quantify the effect of these chosen groups in controlling the structure and dynamics of water molecules simultaneously confined within the hydrophobic pore.

Using the model FCNTs as discussed above, we would like to address several issues on the structure and dynamics of water in hydrophobic confinement. Will the presence of an additional group inside the core disrupt or facilitate the formation of one-dimensional, ordered water chains across the tube? Will they be able to mimic the gating action observed in biological channels? It would also be interesting to know if the chemical identity and physical dimensions of the group attached to the inner wall may affect the structural ordering and residence times of inner water molecules along the tube. We would also like to understand if such endohedral functionalization in SWCNTs of varying lengths may help in retaining the inner water molecules within the tube for a longer time. Although several studies have focussed on using CNTs as mediators for fluid and ion transport, to the best of our knowledge, its use as a prototype for fluid storage has not been explored so far.[9] Our present work will also be directed towards rationalizing the use of endohedrally functionalized SWCNTs as viable templates for storage of water and other fluids. The field exerted by the analogues of polar amino acid sidechains inside the hydrophobic core of SWCNTs has already been shown have substantial effect on the reactivities, energetics, and free energies of simple reactions.[30,31] Therefore, it is not unreasonable to expect interesting variations in the behaviour of water with different functional groups attached to the core of FCNTs.

II. METHOD

We have carried out a series of classical molecular dynamics simulation studies using AMBER12[32,33] on pristine, SWCNT and some of its endohedrally functionalized derivatives. Different steps involved in these studies are outlined below.

A. Generation of initial structures

As discussed earlier,[30] initial structures of single-walled carbon nanotubes with or without endohedral functionalization were obtained in the gas phase using the utilities of DMol3[34] and optimized using density functional theory methods.[35] In the first stage of our work, we have studied pristine (6, 6) open-ended SWCNT of length 15.6 Å and diameter of 8.2 Å. The wall of CNT is a lattice composed of 144 sp^2 hybridized carbon atoms. One such C-atom near the center of the tube was modified into sp^3 hybridized one so that a desired functional group may be covalently attached to it. The functional groups investigated in this work have been chosen to mimic the sidechains of polar amino acid residues such as histidine (His), aspartic acid (Asp), glutamic acid (Glu), threonine (Thr), and serine (Ser). It may be noted that all the sidechains analogues studied here are electrically neutral

and the group suspended from the wall does not contain the peptide linkage generally associated with amino acid structures. Therefore, the sp^3 hybridized C-atom on the wall may be assumed to approximate the C_α-atom of an amino acid residue.

We have also generated FCNTs of length 20.0, 29.9, and 51.9 Å for the system with Asp- and Glu-like sidechains and used them in the last stage of our work. To keep the notations simple, we shall refer to these lengths studied as 15, 20, 30, and 50 Å in the rest of this article.

B. Simulation procedure

All the simulations reported in this work were carried out in a cuboidal box having box lengths of 55, 55, and 60 Å. Each simulation box contained around 5000 TIP3P[36] water molecules. A harmonic potential of 10 kcal mol^{-1} was used in each simulation run to restrict the motion of C-atoms belonging to the nanotube. However, no such restriction was imposed on the atoms of the side chain analogues so that they could fluctuate inside the tube core around their point of suspension from the wall. Interactions between various atoms were modeled by classical AMBER *ff12SB* force field.[32] Carbon atoms constituting the CNT wall were modeled as uncharged Lennard-Jones particles with parameters chosen to fit sp^2 hybridization, while the C_α-like atom was assigned Lennard-Jones parameters suitable for sp^3 hybridization. The partial charges on the atoms of neutral amino acid side chain were taken from the AMBER library file.[32]

Each of the simulation systems, generated as described above, was subjected to energy minimization in two stages. First, minimization was carried out by imposing a harmonic constraint on all atoms belonging to the CNT including those of the side chains. This was followed by an all atom minimization where no restriction as mentioned above was used. In each of these two stages, 50 000 steps of minimization were carried out with first 5000 steps using steepest descent method and the rest using conjugate gradient method.

The minimized structure was subsequently heated slowly from 0 K to room temperature (300 K) and equilibrated in two steps of short (0.5 − 1 ns) *NVT* and *NPT* molecular dynamics simulations, employing $p = 1$ atm in the second case. At the end of these equilibration runs, the box dimensions settled at around 51, 51, and 57 Å for each system. Then *NVT* simulations were carried out for 30 ns using a time step of 2 fs. The temperature was regulated using Langevin dynamics with a collision frequency 5 ps^{-1}. SHAKE algorithm was applied to constrain bonds involving hydrogen atoms. Minimum image convention was employed to calculate short range Lennard-Jones interactions using a spherical cut-off distance of 12 Å. The long range electrostatic interactions were calculated using particle-mesh Ewald (PME) method.[37]

The equilibrated *NVT* MD trajectories were saved at an interval of 400 fs. The configurations sampled during the last 20 − 30 ns of these trajectories were used to calculate structural and dynamic properties of confined water in SWCNT and different FCNTs. In addition, in each simulated system, a separate *NVT* MD trajectory of length of 25 ps was generated using a time step of 0.5 fs from an equilibrium configuration extracted at 20 ns of the longer trajectory. This trajectory was saved every 5 fs, thus allowing us to probe correlated dynamical fluctuations at sub-picosecond time scales.

C. Analysis of equilibrium and dynamical properties

As a first step to investigate structural and dynamical properties of water molecules inside FCNT, the following convention was adopted to identify *inner water molecules* located inside the nanotube. First, for every structure, we define the midpoint of each open end of the tube by connecting two diametrically opposite atoms forming the edge. The two midpoints thus obtained are connected by a straight line which by construction, happens to coincide with the axis of the tube. A water molecule is defined to residing within the tube if the perpendicular distance of its oxygen atom from this straight line happens to be less than half of the CNT diameter. The number of inner water molecules, N_{int} at a given time will be used to compare the water retention capability of the corresponding structure. In addition, we also estimate in each case N_s, the number of *stable* inner water molecules that are retained inside the nanotube more than 99% of the time along the simulated dynamical trajectory.

To identify if a pair of sites on two water molecules are hydrogen bonded or not, we have used in our work the geometry based criteria.[38–41] Accordingly, a pair of site is hydrogen bonded if (a) the inter-oxygen distance, d_{O-O} is less than 3.5 Å, (b) the distance between donor hydrogen and acceptor oxygen, d_{O-H} is less than 2.5 Å, and (c) the angle between donor O–H vector and donor-acceptor O–O vector, θ is less than 30°. As water molecules inside CNTs forms a one-dimensional chain, the equilibrium distribution of water molecules around a given sidechain suspended within the tube has been described in terms of radial distribution functions such as $g_{O-O}(z)$ and $g_{X-O}(z)$. By calculating $g_{O-O}(z)$ between the oxygen atoms (OW) of inner water molecules, we expect to probe how their pair distribution depends on the identity of the suspended functional group in close proximity. On the other hand, we denote oxygen/nitrogen atoms(s) on the side chain that are capable of forming hydrogen bond with the inner water molecules as X. In the present study, the following atoms have been designated as X:

a. the sole oxygen atom (O_γ) of Thr- and Ser-like sidechains,
b. two terminal carboxylic oxygen atoms ($O_{\gamma 1}$, $O_{\gamma 2}$ in Asp and $O_{\epsilon 1}$, $O_{\epsilon 2}$ in Glu) in Asp- and Glu-like sidechains,
c. two nitrogen atoms on the imidazole ring ($N_{\delta 1}$ and $N_{\epsilon 2}$) of His sidechain.

Following the convention introduced above, $g(z)$ has been defined as

$$g(z) = \frac{\rho_z}{\rho_0^{1/3}}, \tag{1}$$

where ρ_z is the number of oxygen atoms (OW) present per unit z at a distance z from a reference atom (X or OW). ρ_0 is bulk density of water. We have also computed first solvation shell inside tube as $\overline{N}_X = \rho_0^{1/3} \int_0^{z_{min}} g(z)dz$. Here, ρ_0 is the

solvent density and distance, z is measured, for example, between O_γ atom of Thr-like sidechain and OW atom of a water molecule residing within the tube. The upper limit chosen to be distance, z_{min} at which the first minimum appears beyond the first peak of $g_{X-O}(z)$.

In order to understand the properties of the sidechain suspended inside the core, we first analyze the distance, $d_{C_\alpha X}$ between C_α and X. In case of His, Asp, and Glu, this distance is monitored by choosing the farthest one of the two X atoms available. We have also probed the tilt angle, θ_t to describe the preferential orientation of the sidechain, if any. θ_t is defined as the angle between the tube axis (z) and the vector connecting the C_α and X, chosen as above. The averages of these quantities are obtained by sampling the relevant dynamical trajectories.

In the present work, we have also estimated an equilibrium distance, $d_{z,t}$ that is measured from the center along the z-axis of the tube. $d_{z,t}$ approximately corresponds to an average distance from the center of the tube where a transition takes place in the average environment of water from a hydrophobic tube-like confinement to the three-dimensional arrangement of bulk polar water. In order to estimate $d_{z,t}$, we first calculate the local tetrahedral order parameter q_{tet} associated with an atom i of a water molecule that is defined as

$$q_{tet} = 1 - 3/8 \sum_{j=1}^{3} \sum_{k=j+1}^{4} (\cos \psi_{jk} + 1/3)^2, \tag{2}$$

where ψ_{jk} is the angle between bond vectors r_{ij} and r_{ik}, where j and k label the four nearest neighbour atoms of the same type.[42–44] This parameter is well known in bulk water and a wide range of aqueous systems.[45–50] The distance along z-axis, at which q_{tet} attains the bulk water value, is equated to $d_{z,t}$ and used later in our analysis.

The dynamical properties of water inside the FCNT have been characterized in terms of the following time correlation functions.

(a) ***Continuous residence time correlation function***, $C_R(t)$ is defined as

$$C_R^{(n)}(t) = \frac{\langle r_n(0) R_n(t) \rangle}{\langle r_n(0) r_n(0) \rangle}. \tag{3}$$

The residence functions, r and R, are defined in terms of the number of inner water molecules, n that are present at a time t. Correspondingly, to estimate the residence time of a single water molecule within the nanotube core, we set $r_1(0) = 1$ if a tagged water molecule is located inside the tube at $t = 0$. $R_1(t) = 1$ if a tagged water molecule continuously remains inside the CNT from $t = 0$ up to $t = t$; $R_1(t) = 0$ otherwise. We have also used Eq. (3) to probe the residence times associated with a tagged pair ($n = 2$) or larger number ($n > 2$) of water molecules residing simultaneously inside the core for different CNT-based systems. $C_R^{(n)}(t)$ is thus expected to reveal the lifetime of join occurrence of n water molecules inside the core by averaging along the entire dynamical trajectory for a given system.

(b) ***Intermittent H-bond time correlation function***, $C(t)$ is defined as

$$C(t) = \frac{\langle h(0) h(t) \rangle}{\langle h(0) h(0) \rangle}. \tag{4}$$

Here, $h(t) = 1$ if a particular pair of site is H-bonded at time t, otherwise it is 0. $C(t)$ is independent of possible breaking and reformation of hydrogen bond within the time interval 0 to t. Angular brackets denote that calculations are averaged over all hydrogen bonds formed at different initial times.

(c) ***Continuous H-bond time correlation function***, $S(t)$ is defined as

$$S(t) = \frac{\langle h(0) H(t) \rangle}{\langle h(0) h(0) \rangle}. \tag{5}$$

Here, $h(0)$ is 1 if a given pair of sites is hydrogen bonded at time $t = 0$, otherwise it is 0. If the tagged pair is hydrogen bonded continuously from $t = 0$ up to $t = t$, $H(t) = 1$. Otherwise it is 0.

(d) ***H–H vector auto time correlation function***, $C_{HH}(t)$ is defined as

$$C_{HH}(t) = \frac{\langle \vec{v}(0).\vec{v}(t) \rangle}{\langle \vec{v}(0).\vec{v}(0) \rangle}, \tag{6}$$

where $\vec{v}(t)$ is vector connecting the two H-atoms within a given inner water molecule at time t.

For each of the correlation functions listed above, the relaxation time, $\langle \tau \rangle$ is calculated by fitting the correlation function, $C(t)$, for example, to a sum of three exponentials as $C(t) = \sum_i a_i \exp(-t/\tau_i)$ so that $\langle \tau \rangle = \int_0^\infty dt C(t)$.

III. RESULTS AND DISCUSSION

We shall describe in Secs. III A–III D the results of our simulation studies on pristine SWCNT and its five different endohedrally functionalized derivatives for each of which the nanotube length is 15.6 Å. The dependence of our results on the nanotube length has been explored for Asp- and Glu-FCNTs in Sec. III E.

A. Retention of water molecules inside the nanotube

Typical representations of water molecules inside pristine and functionalized CNTs (with the nanotube length of 15.6 Å) are shown in Fig. 1, where, for the sake of clarity, only inner water molecules have been highlighted. In all the cases studied, we observe the formation of water chains of varying length and duration, extending through the core of the tube, distributed asymmetrically on both sides of the sidechain.

We present in Fig. 2 the average number of inner water molecules, $\bar{N}_{int}$ present for the pristine SWCNT as well as for its five different functionalized derivatives. This number has been estimated in each case by considering the last 20 ns of the relevant simulated trajectories. We have also highlighted in the same figure the number of stable water molecules, N_s that are retained within the tube for more than 99% of the length of our simulated trajectory. It is clear from our results that both $\bar{N}_{int}$ and N_s depend crucially on the identity of the sidechain extending into the core. Asp-, Glu-, and

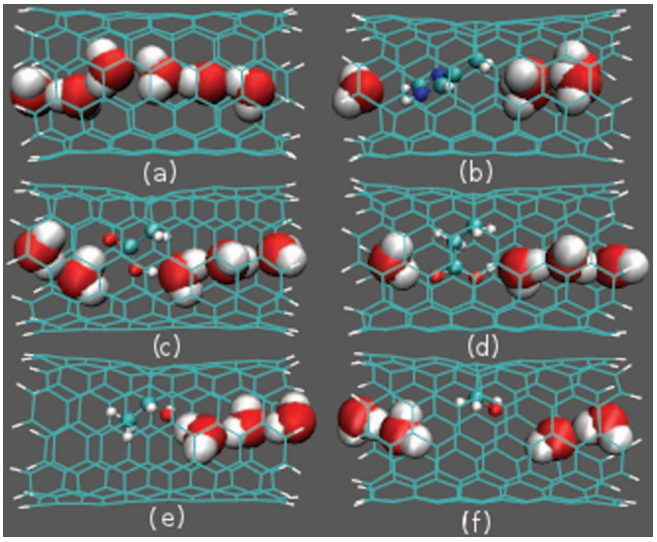

FIG. 1. Representative structures of the simulated pristine and functionalized SWCNTs: (a) Pristine CNT, (b) His-FCNT, (c) Asp-FCNT, (d) Glu-FCNT, (e) Thr-FCNT, (f) Ser-FCNT. Water molecules solvating the system in the simulation box have not been shown.

Ser-like sidechains are associated with the retention of more than 4 inner water molecules on an average. Of these, 3 water molecules in Asp-FCNT are found in *all* the snapshots of the simulated trajectory. In contrast, of the 3 stable water molecules are identified in Glu-FCNT, one was found to remain inside all throughout the trajectory while the other two were transiently removed from the core in about 1% of the structures sampled. Thr-FCNT similarly has 2 stable water molecules, out of which only one is retained inside all along the trajectory. Interestingly, neither His-FCNT nor Ser-FCNT yield any such long-lived water molecules inside the tube, in close resemblance to the pristine CNT.

To extend the scope of our definition of *stable* water molecules, we further investigated the distribution, $f(N_{int})$ of N_{int} for different FCNTs and the results are shown in Fig. 3. Clearly, $4-6$ water molecules dynamically reside within the

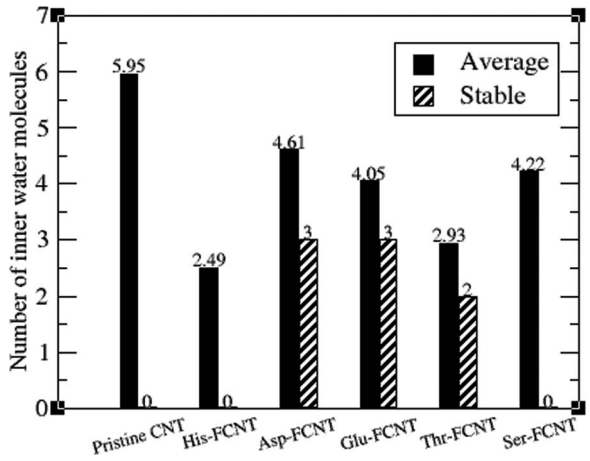

FIG. 2. Estimated number of inner water molecules in pristine and functionalized CNTs. The solid boxes represent the average number, $\bar{N}_{int}$ while the striped boxes correspond to the number of stable water molecules N_s, defined as those residing within the nanotube all throughout the sampled trajectory.

pristine CNT with $N_{int} = 5$ for more than 70% of the structures sampled. In Glu-FCNT, only one dominant peak is observed at $N_{int} = 4$ corresponding to 4 inner water molecules in more than 70% of the structures sampled. Although the most preferred value of N_{int} is 4 in Asp-CNT, a substantial fraction of its structures can accommodate 5 inner water molecules. $\bar{N}_{int}$ in Asp-FCNT is thus larger than that in Glu-FCNT. Ser-FCNT shows the widest range of values for N_{int}. The distributions observed in His- and Thr-FCNTs are mostly centered around $N_{int} = 2-3$ with relatively lower preferences for any specific value. The observed difference in $\bar{N}_{int}$ and N_s is easily attributed to the entry/exit of inner water molecules at the two terminals of the nanotube.

B. Inner water molecules around the suspended group

Let us next examine the role of different suspended groups on the number and fluctuation of inner water molecules. On account of the finite excluded volume associated with the sidechain analogue suspended within the core, $\bar{N}_{int}$ falls short of the average number of nearly six water molecules that can be accommodated inside the pristine SWCNT having the same dimensions. Although we designed and optimized our model systems to have the endohedral functionalization as close to the center of the tube as possible, the chemical structure of the suspended group and a finite excluded volume associated with it render the core asymmetric with respect to occupation by water molecules on the two sides of it. The average orientational preferences of the sidechain analogues inside the core are pictorially shown in Fig. 4 and the associated average structural data summarized in Table I. It is found that $d_{C_\alpha X}$ is larger in His- and Glu-like sidechains and is smallest in Thr- and Ser-like sidechains. The distributions of tilt angle, θ_t, presented in Fig. 5 for all the FCNTs, reveal the different orientations sampled by different groups inside the core. For each of these FCNTs, we have also examined if the available inner core volume is distributed equally on the two sides of the sidechain and the results are shown in Fig. 5 and Table I. All these contribute to result in the following order for the average number of inner water molecules: $\bar{N}_{int}$: $His-FCNT < Thr-FCNT < Glu-FCNT < Ser-FCNT < Asp-FCNT$.

Correlating the values of N_{int} with the asymmetric distribution of water molecules around the suspended group, the following *average* scenario emerges. The His-like sidechain is found to be predominantly tilted to one side effectively blocking that side of the hydrophobic core from occupation by any stable or relatively long-lived water molecule. Both Asp- and Glu- like sidechains sample orientations around 90° (although in opposite directions) thereby allowing similar asymmetric environment to the approaching inner water molecules. For Asp-FCNT, we thus observe 2 stable water molecules on one side with only one such stable one on the other side of the suspended sidechain. The longer sidechain of Glu-FCNT disturbs the distribution of available core volume for occupation by inner water molecules marginally compared to Asp-FCNT. However, even such small changes could lower the retention time of two of its 3 stable water molecules. The

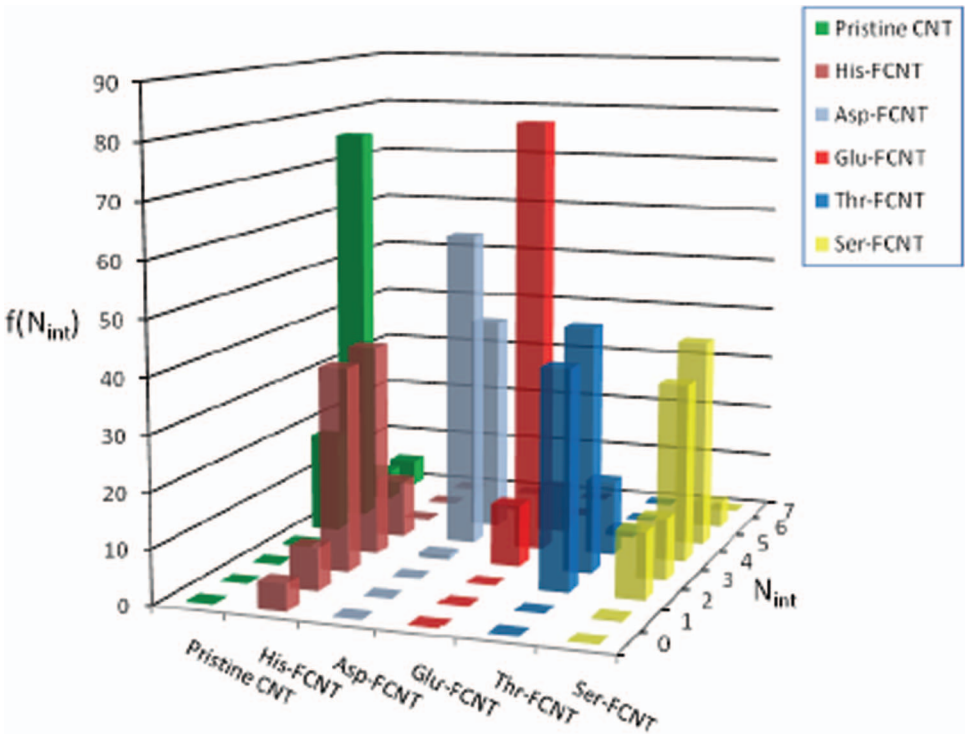

FIG. 3. Distribution of the number of inner water molecules, $f(N_{int})$ present in pristine CNT and FCNTs.

Ser-like sidechain, on the other hand, exhibits dynamical fluctuations sampling at least three sets of orientational conformers of which two are tilted and one is nearly perpendicular with respect to the tube axis. These fluctuations drive faster expulsion of inner water molecules from the nanotube compared to Asp- or Glu-FCNTs. The Thr-like sidechain, in spite of having $d_{C_\alpha X}$ values comparable to that of Ser, remains more tilted and sample a narrower range of orientations due to the presence of a hydrophobic $-CH_3$ group on it. Moreover, on account of the tilted orientation of the suspended group, the distribution of water molecules on its two sides turns out to be highly asymmetric. For example, two water molecules are mostly found to be within hydrogen bonding distance to the Thr-like sidechains on the face having its O_γ atom. But only one such water molecule is detected near its face with the methyl group that remains relatively devoid of long-lived water molecules.

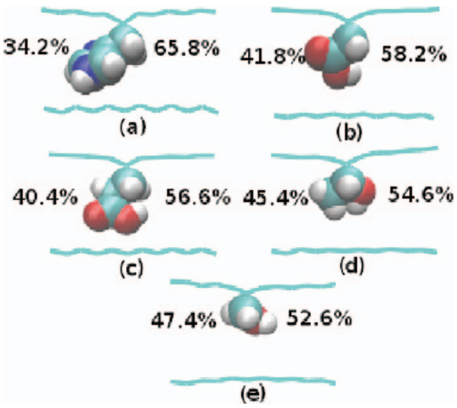

FIG. 4. Average orientations of the analogue of amino acid sidechain in different FCNTs: (a) His-FCNT, (b) Asp-FCNT, (c) Glu-FCNT, (d) Thr-FCNT, and (e) Ser-FCNT. The value shown on each side of the suspended group corresponds to the percentage of f_{wat}, fraction of the inner core volume that can be occupied by inner water molecules.

C. Equilibrium correlations

We next probe the extent to which the presence of a suspended group may affect the equilibrium correlation between the inner water molecules in the FCNTs along the tube axis (z-axis). We have shown in Fig. 6 different distribution functions, $g_{OW-OW}(z)$ obtained from our simulations. Table II summarizes the estimated values of z_{max} and z_{min}, at which the first maximum and minimum of $g_{OW-OW}(z)$ appear, respectively.

TABLE I. Average structural data on the relative sizes and orientations of suspended analogues of amino acid sidechains (SCs) in different FCNTs (of length 15.6 Å) and volumes available for occupation by inner water molecules. [$d_{C_{\alpha-X}}$: distance between C_α and the farthest heteroatom, X on the SC that is capable of forming hydrogen bond with water; θ_t: tilt angle; f_{wat}: fraction of core volume available for occupation by inner water molecules.]

FCNTs	$C_\alpha - X$ pair	$\overline{\theta}_t$ (deg)	$\overline{d}_{C_{\alpha-X}}$ (Å)	f_{wat}	% of f_{wat} on the left of SC	% of f_{wat} on the right of SC
His-FCNT	C_α–$N_{\epsilon 2}$	123.8	4.5	0.9	34.2	65.8
Asp-FCNT	C_α–$O_{\delta 2}$	99.4	3.9	0.9	41.8	58.2
Glu-FCNT	C_α–$O_{\epsilon 2}$	89.4	4.5	0.9	40.4	56.6
Thr-FCNT	C_α–O_γ	66.1	2.5	0.9	45.4	54.6
Ser-FCNT	C_α–O_γ	81.0	2.6	1.0	47.4	52.6

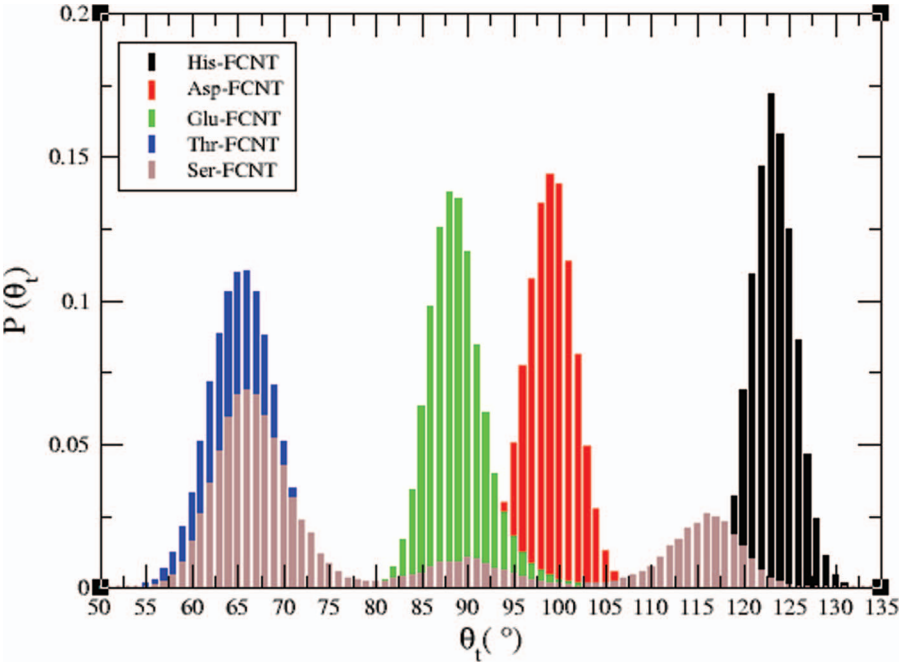

FIG. 5. Distribution of the tilt angle, θ_t of the endohedrally suspended group inside the nanotube core for (a) His-FCNT (black, around 125°), (b)Asp-FCNT (red, around 100°), (c) Glu-FCNT (green, around 87°), (d) Thr-FCNT (blue, around 65°), and (e) Ser-FCNT (grey, around 65°, 90°, and 117°).

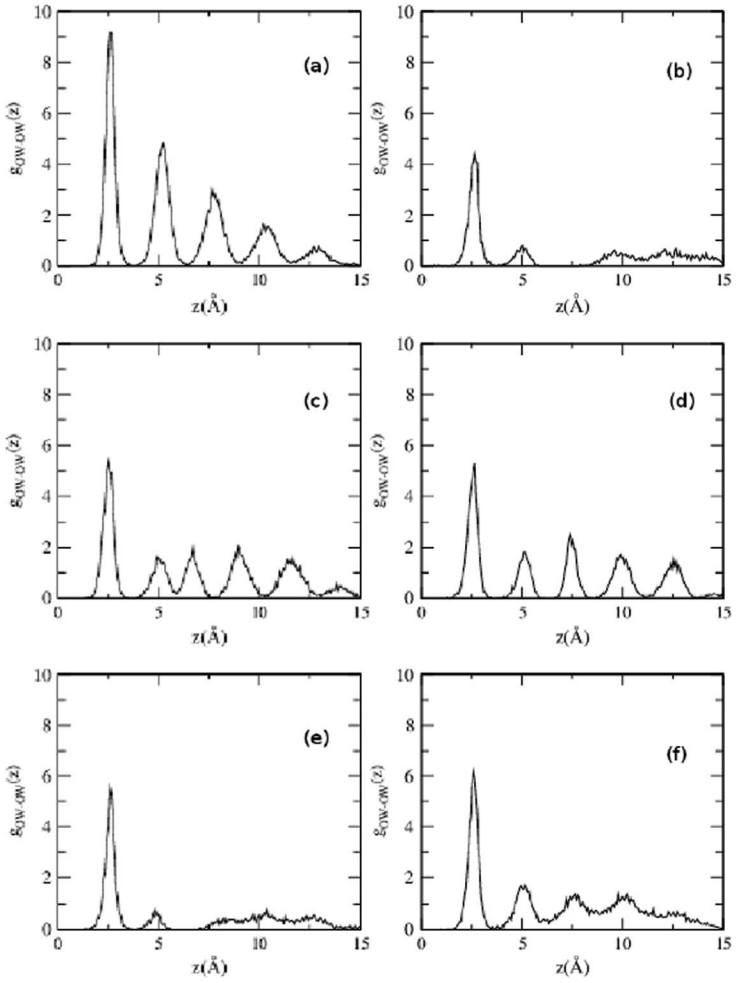

FIG. 6. OW-OW pair correlation functions of inner water molecules in (a) pristine CNT, (b) His-FCNT, (c) Asp-FCNT, (d) Glu-FCNT, (e) Thr-FCNT, and (f) Ser-FCNT.

TABLE II. Equilibrium pair correlation function $g_{OW-OW}(z)$ between inner water molecules in terms of the location (z_{max}) and peak height, $g(z_{max})$ of its first maximum, location of the first minimum (z_{min}), and average coordination number, $\overline{N}_O$ in the first solvation "shell."

System	z_{max} (Å)	$g(z_{max})$	z_{min} (Å)	$\overline{N}_O$
Pristine CNT	2.6	9.2	3.8	1.7
His-FCNT	2.7	4.4	3.7	0.9
Asp-FCNT	2.5	5.4	3.6	1.1
Glu-FCNT	2.7	5.3	3.7	1.0
Thr-FCNT	2.6	5.5	3.8	0.9
Ser-FCNT	2.6	6.2	3.6	1.1

Highly ordered, solid-like structures of water molecules are formed not only in pristine CNT, but also in the presence of −COOH group of Asp- and Glu-like sidechains. In both these cases, the presence of two oxygen atoms on the −COOH group ensures the formation of a continuous and tightly held water chain extended across the nanotube. Insertion of the sidechain in a FCNT does decrease the nearest OW–OW correlation compared to the pristine CNT. This is evident from lower values of first peak height, $g(z_{max})$ in the FCNTs whereby 67%, 58% − 60%, and 47% of the pristine $g(z_{max})$ values are retained in the presence of Ser-, Thr-/Asp-/Glu-, and His-like sidechains, respectively. Persistence of the water chain inside the tube away from the sidechain is indicated clearly by the appearance of several CNT-like peaks for $z > z_{max}$. The length z_{min} corresponds to the average distance between OW atoms within their first solvation *shell*. As shown in Table II, it varies between 3.6 and 3.8 Å, falling slightly shorter than that estimated in pristine CNT (3.84 Å). FCNTs with His-, Thr-, and Ser-like sidechains, on the other hand, do not exhibit any such long range ordering of inner water molecules among themselves. The tail-like correlation for large values of z in all these cases appears mainly because of fluctuations in the number of water molecules at the open ends of the nanotube. The presence of a methyl group on the Thr-like sidechain appears to make it less efficient in facilitating the OW–OW correlation compared to a Ser-like sidechain. Evidently, the number and nature of hydrogen bonding sites, X as well as the space excluded by the side chains contribute to its ability to alter the micro-environment inside the nanotube core.

The asymmetry in water distribution around the sidechain has been highlighted in Fig. 7 by plotting the pair distribution, $g_{X-OW}(z)$ as a function of the separation z between X and OW of an inner water molecule. The position and height of the first peaks as well as z_{min} have been summarized in Table III for all the FCNTs. The correlation observed is strongest in the case of Asp- and Glu-like side chains with the acidic oxygen atoms stabilizing well-localized inner water molecules up to a separation of $z = 10$ Å. In Thr- and Ser-FCNTs, strong correlations are observed consistent with our earlier observations as in Fig. 6. However, the peaks are fewer in number and markedly broader in these cases compared to Asp- and Glu-FCNT. This implies that the −OH group can control the ordering of only a couple of inner water molecules with less efficient localization than the −COOH group. It is interesting to note that Ser-FCNT produces sharp peaks in close resemblance to Asp/Glu-FCNT indicating the formation of extended inner water chains. However, direct connectivity of the $-CH_2$ group to X = O_γ of Ser-like sidechain is found to affect formation of these long-range water chains. In conformations where the $-CH_2$ group interposes itself between O_γ and the O-atom of an inner water molecule, the water chain gets disrupted. Conformations lacking such hindrance are found to be associated with a well formed water chain across the nanotube. The last peak in each case is broader than the peaks observed at short ranges. This once again correlates with the exchange between water molecules within CNTs and the surrounding of water molecules in bulk.

The estimated coordination numbers, $\overline{N}_X$ for different FCNTs are shown in Table III. It is found that $\overline{N}_X = 1$ for each X in all FCNTs except Ser-FCNT where $\overline{N}_X$ of the O_γ atom turns out to be close to the coordination number of 1.66 of an inner water molecule in pristine CNT.

In Fig. 8, we have shown the plot of q_{tet} as a function of displacement z from the center of the tube along its axis. As expected, the average environment of water molecules located within the CNT shows marked deviation from the tetrahedral ordering of bulk. The effect of hydrophobic confinement is found to extend beyond the limits of the tube. Importantly, for the FCNTs, the effect of confinement is sustained up to 10 Å along z-axis from the center of tube after which a bulk-like value of q_{tet} sets in. Correspondingly, $d_{z,t}$ is estimated to be 10 Å.

D. Dynamical properties

In Fig. 9, the relaxation of residential correlation functions, $C_R^1(t)$ for different simulated systems are highlighted and the corresponding average residence times, $\langle\tau_R\rangle$ have been presented in Table IV. It is evident from the figure that the residence time of a single water molecule inside the CNT is shortest for the pristine CNT and His-FCNT. The average residence times of an inner water molecule in these two systems are 135.9 and 127.1 ps, respectively. It is important to note that 2 − 3 water molecules coming in from one side of the nanotube in His-FCNT do reside inside the tube for some time. However, as mentioned earlier, lack of water molecules residing on the other side of the sidechain causes $\langle\tau_R\rangle$ of His-FCNT to be even smaller than that of pristine CNT. The decay rates of $C_R^1(t)$ of water molecules inside Asp-FCNT and Glu-FCNT are found to be the slowest with the time constants 4.1 and 3.5 ns, respectively. We also note a much smaller value of $\langle\tau_R\rangle = 572.9$ ps in Ser-FCNT compared to that of Thr-FCNT $\langle\tau_R\rangle = 1.1$ ns. This may be primarily attributed to the following. Although a hydrogen bonded water chain mediated by the −OH group of Ser is easily formed, sidechain conformational fluctuations of Ser disrupt this chain as soon as its methylene group comes in close proximity to the bridging water molecules. Correspondingly, the average residence time, $\langle\tau_R\rangle$ of water molecules in Ser-FCNT becomes much smaller compared to Thr-, Asp-, or Glu-FCNT. It may also be noted that τ_1, longest of the three time constants used to estimate $\langle\tau_R\rangle$, is expected to correspond to those water molecules closest to X inside the nanotube.

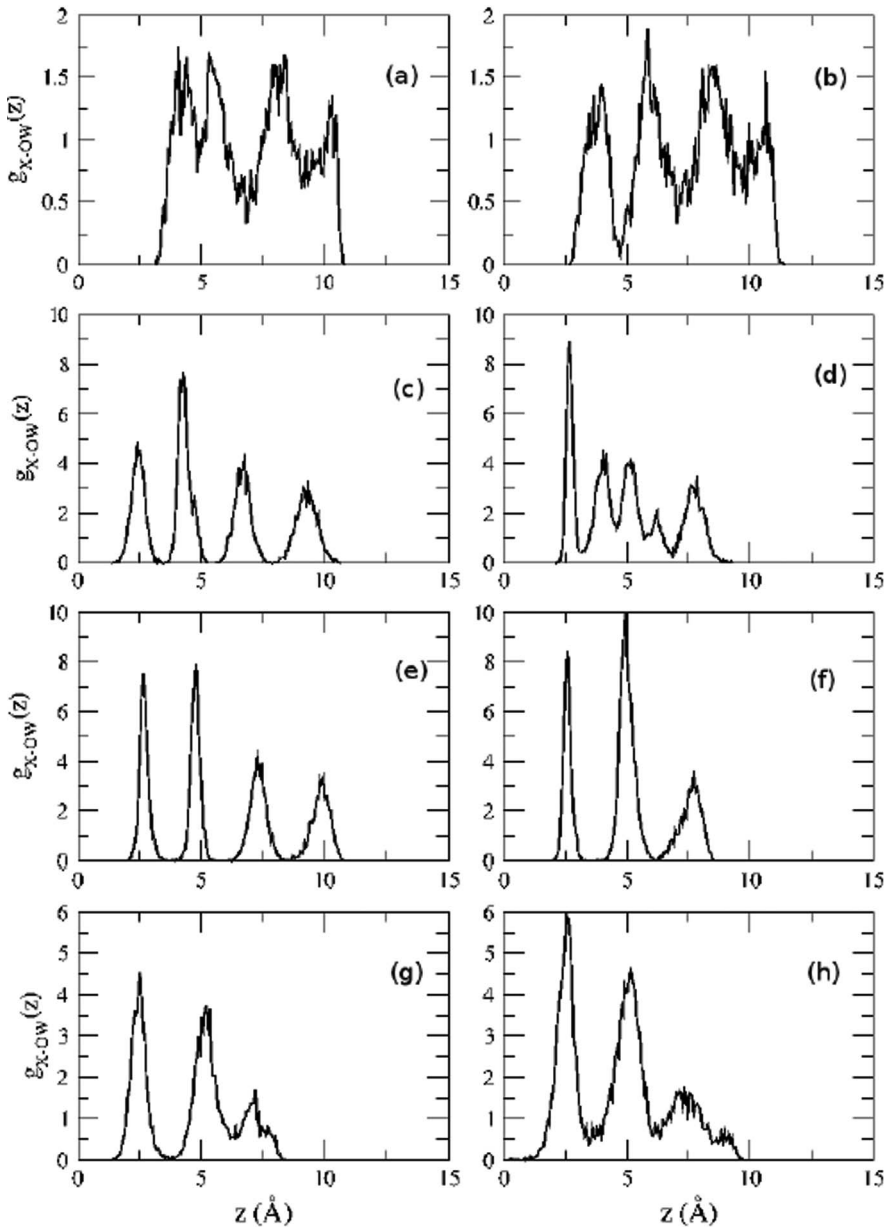

FIG. 7. X-OW pair correlation functions in (a) His-FCNT ($N_{\delta 1}$–OW), (b) His-FCNT ($N_{\epsilon 2}$–OW), (c) Asp-FCNT ($O_{\delta 1}$–OW) (d) Asp-FCNT ($O_{\delta 2}$–OW), (e) Glu-FCNT ($O_{\epsilon 1}$–OW), (f) Glu-FCNT ($O_{\epsilon 2}$–OW), (g) Thr-FCNT (O_{γ}–OW), (h) Ser-FCNT (O_{γ}–OW).

TABLE III. Equilibrium pair correlation function $g_{X-OW}(z)$ between the sidechain atom X and an inner water molecule in terms of the location (z_{max}) and peak height, $g(z_{max})$ of its first maximum, location of the first minimum (z_{min}), and average coordination number, $\overline{N}_X$ in the first solvation "shell."

FCNTs	X − OW pair	z_{max} (Å)	$g(z_{max})$	z_{min} (Å)	$\overline{N}_X$
Asp-FCNT	$O_{\delta 1}$–OW	2.4	4.9	3.5	1.0
	$O_{\delta 2}$–OW	2.7	8.9	3.3	1.0
Glu-FCNT	$O_{\epsilon 1}$–OW	2.7	7.3	3.7	1.0
	$O_{\epsilon 2}$–OW	2.6	8.5	3.3	1.0
Thr-FCNT	O_{γ}–OW	2.5	4.5	3.7	1.0
Ser-FCNT	O_{γ}–OW	2.6	5.6	3.5	1.6

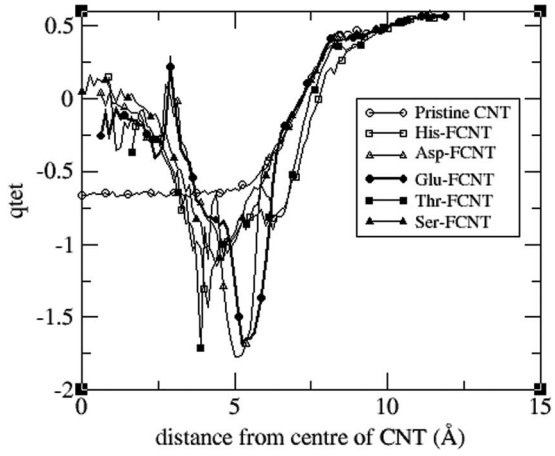

FIG. 8. Tetrahedral order parameter, q_{tet} of an inner water molecule monitored up to 10 Å along z-axis from the center of the nanotube.

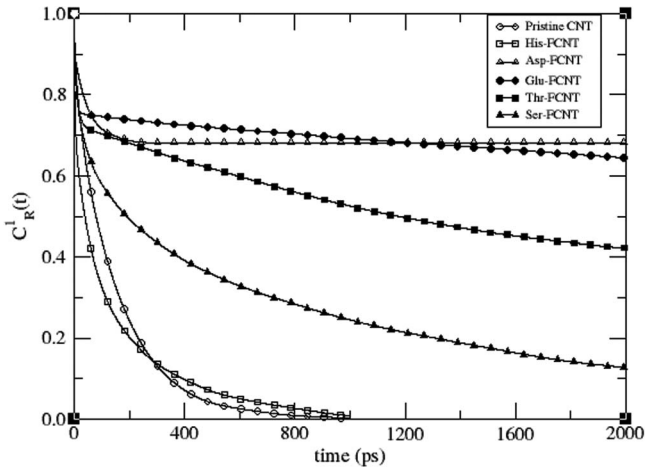

FIG. 9. Relaxation of the residential time correlation function, $C^1_R(t)$ in (a) pristine CNT (○), (b) His-FCNT (□), (c) Asp-FCNT (△), (d) Glu-FCNT (●), (e) Thr-FCNT (■), and (f) Ser-FCNT (▲).

In order to determine the values of N_{int} that correspond to the longest surviving water molecules coexisting inside the core for the given dimensions of the nanotube (length L = 15.6 Å), we have shown in Fig. 10 the residence times, $\tau_R(N_{int})$ for different N_{int} in all the simulated systems studied here. It is found that the pristine CNT can host 6 inner water molecules continuously for up to about 3 ps. The large peak observed at $N_{int} = 0$ for His-FCNT corresponds to a large fraction of the sampled structures having no inner water molecules inside the core. At best, His-FCNT could accommodate 2 water molecules (both present on the same side of the suspended group) for up to 1.78 ps. Both Glu- and Asp-FCNTs are capable of retaining 4 water molecules simultaneously up to 3.02 and 1.33 ps, respectively. Rapid exchange of an average of one water molecule on each side of the suspended group at the open mouth of the nanotube lowers the residence time of each water molecule on the whole. In Ser- and Thr-FCNTs, a maximum of 2 water molecules are held inside simultaneously for 2 − 2.5 ps, while 5 water molecules are retained inside for up to 1.5 ps.

The mean square displacements (MSD) along z-axis of all water molecules inside different CNTs are shown in Fig. 11. In Fig. 11(a), we have considered displacement exactly up to end of the tube so that it may be used to estimate the corresponding diffusion coefficient, D_z. On the other hand, as shown in Fig. 11(b), MSD up to $d_{z,t} = 10$ Å has been monitored and the related diffusion coefficient, D'_z calculated. The values of D_z and D'_z thus obtained have been summarized in Table V. As expected, both Asp- and Glu-FCNTs exhibit relatively lower values of D_z with respect to pristine CNT or His-FCNT. Interestingly, the effect of expulsion of water molecules from Glu-FCNT is found to be the strongest with its D'_z value increasing by nearly an order of magnitude over that of D_z. Comparison of the values of diffusion constants to their respective residence times, $\langle\tau_R\rangle$, as shown in Table IV, reveals a non-trivial dependence of these quantities on each other.

TABLE IV. Average residence time, $\langle\tau_R\rangle$ of a water molecule inside the nanotube in pristine and functionalized CNTs of length 15.6 Å.

Systems	Pristine-CNT	His-FCNT	Asp-FCNT	Glu-FCNT	Thr-FCNT	Ser-FCNT
$\langle\tau_R\rangle$ (ps)	135.88	127.14	4096.41	3562.64	1086.77	572.94

To investigate the role of hydrogen bonding on the order of magnitude change in $\langle\tau_R\rangle$, the intermittent time correlation function, $C(t)$ has been estimated considering those formed between inner water molecules themselves and between inner water molecules and the heteroatom(s) X in FCNTs. Result of our calculation of $C(t)$ for different FCNTs are shown in Fig. 12. It is clear from the plot that the relaxation of intermittent hydrogen bonding between inner water molecules is the slowest in Asp- and Glu-FCNTs and fastest in His-FCNT. The average relaxation times of intermittent hydrogen bond time correlation function, $\langle\tau_c\rangle$ are shown in Table VI. $\langle\tau_c\rangle$ are found to become nearly 4 − 7 times in Thr-, Glu-, and Asp-FCNTs than that observed in pristine CNT ($\langle\tau_c\rangle = 69.8$ ps). It is also observed that the −COOH groups of Asp- and Glu-like sidechains are capable of exerting the strongest effect even within a hydrophobic core.

If we do not consider the H-bond between water molecules and the −COOH group of Asp and Glu, the value of τ_c becomes comparatively smaller at 219.38 ps and 172.13 ps, respectively. It implies that strong hydrogen bonding of inner water molecules with –COOH group in turn results in longer lived hydrogen bonding between the inner water molecules compared to the case of pristine CNT ($\tau_c = 63.51$ ps). Once again, in spite of having a polar side chain, the decay rate of $C(t)$ in His-FCNT is faster than others, even faster than the same in pristine CNT.

We next examine the time dependence of the continuous H-bond time correlation function, $S(t)$ by sampling dynamical trajectories of length 25 ps generated with a time step of 0.5 fs. The result for different FCNTs are shown in Fig. 13. It may be noted that the relaxation of a hydrogen bond is found to depend crucially on whether it is OW–OW (between inner water molecules) or X–OW (between X and inner water molecule). We have studied here both the case where (a) only OW–OW H-bonds are considered and (b) where both types of H-bonds are sampled. It is clear that the rate of decay of an individual hydrogen bond does not depend much on the identity of the bonding pair except in the cases of Asp- and Glu-FCNT. Correspondingly, the Asp-like sidechain is found to be capable of holding the water chain longest inside the tube (Table VI). In particular, persistence of a continuous hydrogen bond in the vicinity of Glu- is apparently hindered by the dynamical fluctuations of the additional $-CH_2$ group making its relaxation time much smaller compared to Asp.

We have also investigated H–H vector auto time correlation function, $C_{HH}(t)$ of water molecules to derive a quantitative picture of correlated rotational motion of inner water molecules around their respective dipole moment axis. The variations of $C_{HH}(t)$ for different FCNTs are shown in Fig. 14 and corresponding average relaxation times have been presented in Table VI. It is found that the fastest relaxation mode of the inner water molecules originate from their orientational relaxation about their dipole axis. The relaxation rate

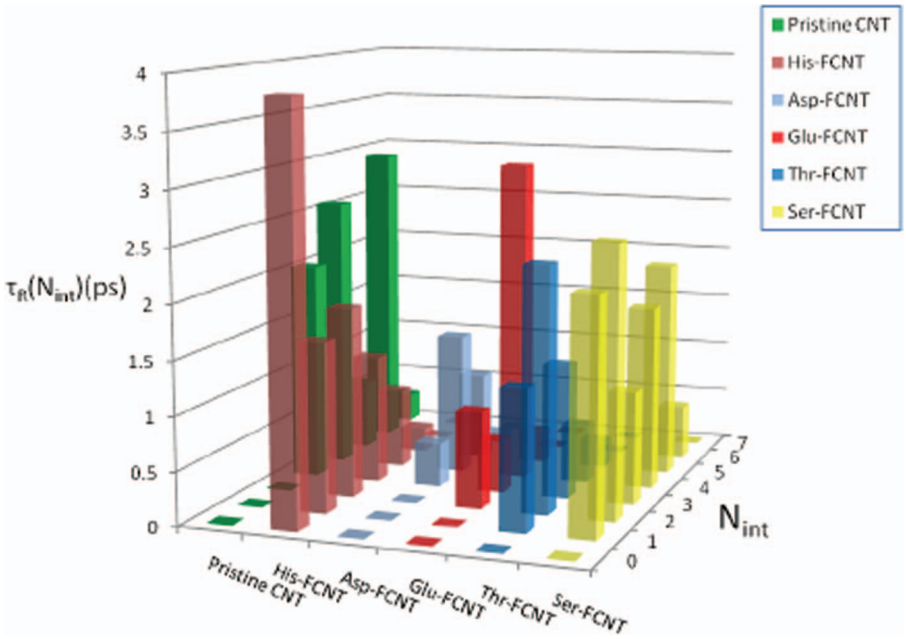

FIG. 10. Residence times of inner water molecules, $\tau_R(N_{int})$ present in pristine CNT and FCNTs as functions of the number of inner water molecules, N_{int}.

is slowest in the case of water molecules inside Asp-FCNT and fastest in the case of His-FCNT. Therefore, these results corroborate well with our earlier observation of long-lived hydrogen-bonded chains in Asp- and Glu-FCNTs.

E. Length dependence of $\langle\tau_R\rangle$ in Asp- and Glu-FCNTs

We have also investigated how the average residence time of a single water molecule varies with the length of CNT. For this purpose, we have chosen only Asp- and Glu-FCNTs on account of the demonstrated ability of these −COOH groups to stabilize longest water chains for a maximum time. The average numbers of water molecules inside the FCNTs, $\bar{N}_{int}$ obtained for 4 different lengths, L of the nanotube, are shown in Fig. 15. As expected, a significant increase is observed for N_s, the number of water molecules being retained inside for the entire length of simulation. The average residence time, $\langle\tau_R\rangle$ is also found to increase with increasing length of the CNT. The temporal decays of $C_R^1(t)$ in Asp- and Glu-FCNTs have been shown in Fig. 16. As noted earlier, an Asp-FCNT of length 15.6 Å can sustain a three-water mediated chain for 20 ns. In contrast, we observe chains comprised of 5, 8, and 16 water molecules in Asp-FCNTs of lengths 20, 30, and 50 Å, respectively, Unlike the periodic purging of water molecules from inside the pristine CNTs, in each Asp-FCNT studied here, the entire water chain is found to preserve itself for the entire 20 − 30 ns of the simulated trajectory. Only terminal two or three water molecules in each case are

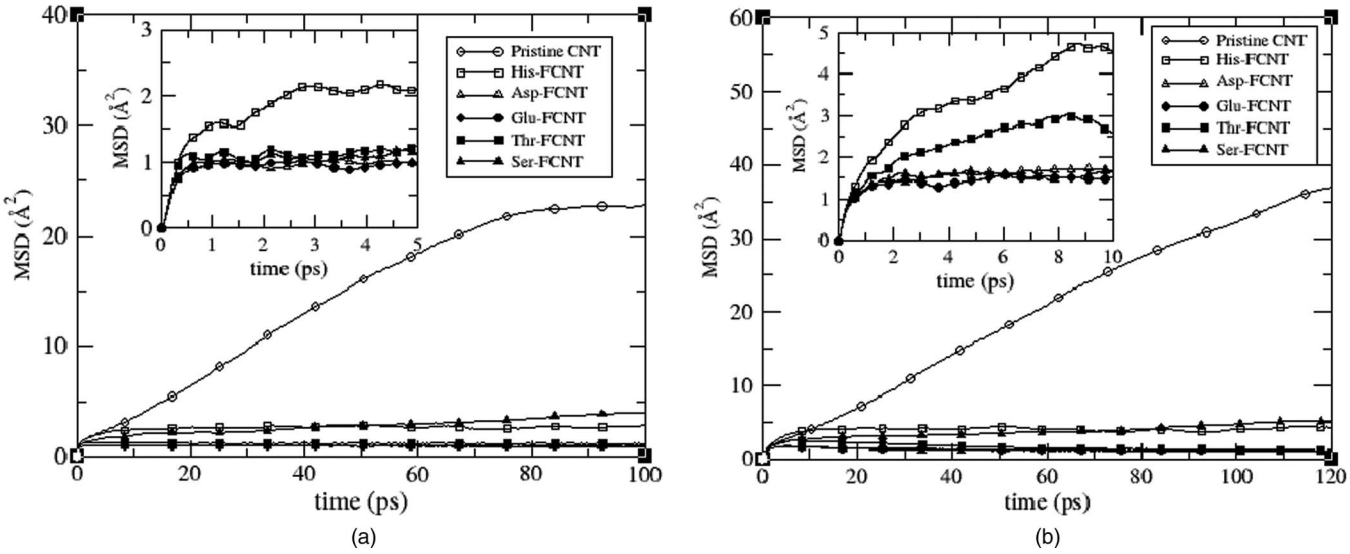

FIG. 11. Mean square displacement of water molecules inside different CNTs measured along the z-axis from the center of the nanotube (a) up to the end of the tube and (b) up to $d_{z,t} = 10$ Å.

TABLE V. Diffusion constant of water molecules inside SWCNT and associated FCNTS, considering displacement along the z-axis up to end of tube, D_z and up to 10 Å along z-axis from the centre of tube, D'_z.

CNTs	D_z (cm^2/s)($\times 10^{-5}$)	D'_z (cm^2/s)($\times 10^{-5}$)
Pristine CNT	1.57	1.72
His-FCNT	1.74	1.45
Asp-FCNT	0.14	0.19
Glu-FCNT	0.01	0.13
Thr-FCNT	0.23	0.85
Ser-FCNT	0.10	0.10

TABLE VI. Average relaxation times, $\langle\tau\rangle$ of different hydrogen bond correlation functions. [$\langle\tau_C\rangle$: for $C(t)$; $\langle\tau_s\rangle_{OW-OW}$: for $S(t)$ considering hydrogen bonding between inner water molecules only; $\langle\tau_s\rangle$: for $S(t)$ considering hydrogen bonds among inner water molecules along with X–OW bonds.] $\langle\tau_{HH}\rangle$ corresponds to the average relaxation times of $C_{HH}(t)$.

CNTs	$\langle\tau_C\rangle$ (ps)	$\langle\tau_s\rangle_{OW-OW}$ (ps)	$\langle\tau_s\rangle$ (ps)	$\langle\tau_{HH}\rangle$ (ps)
Pristine CNT	69.81	0.27	0.27	0.34
His-FCNT	75.68	0.16	0.16	0.28
Asp-FCNT	490.74	0.41	2.04	0.81
Glu-FCNT	462.09	0.45	0.29	0.40
Thr-FCNT	307.07	0.28	0.26	0.33
Ser-FCNT	149.04	0.24	0.26	0.48

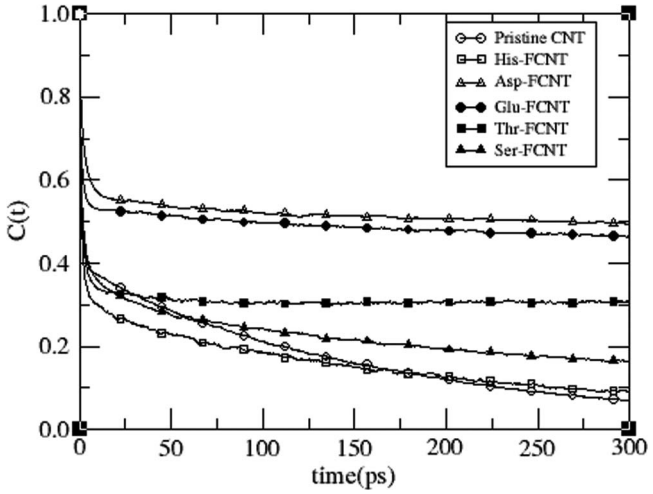

FIG. 12. Time dependence of the intermittent hydrogen bond time correlation function, $C(t)$ in (a) pristine CNT (○), (b) His-FCNT (□), (c) Asp-FCNT (△), (d) Glu-FCNT (●), (e) Thr-FCNT (■), and (f) Ser-FCNT (▲).

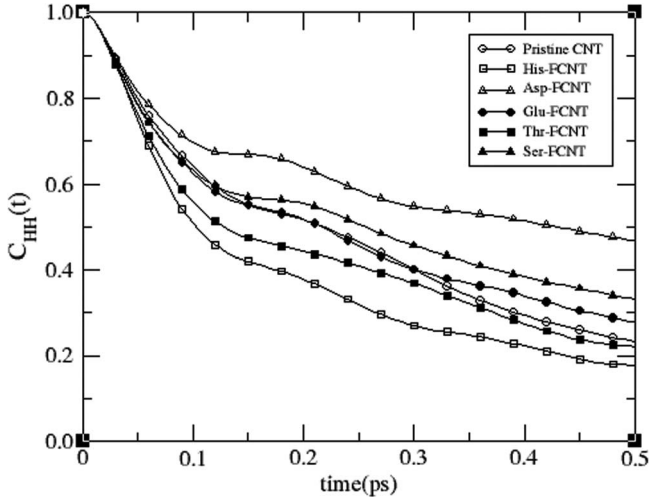

FIG. 14. H–H vector auto time correlation function in (a) pristine CNT (○), (b) His-FCNT (□), (c) Asp-FCNT (△), (d) Glu-FCNT (●), (e) Thr-FCNT (■), and (f) Ser-FCNT (▲).

exchanged with water bath. The additional $-CH_2$ group in Glu-like sidechain seems to make it marginally less efficient than its Asp-like counterpart for retention of a maximum number of water molecules for a largest possible time.

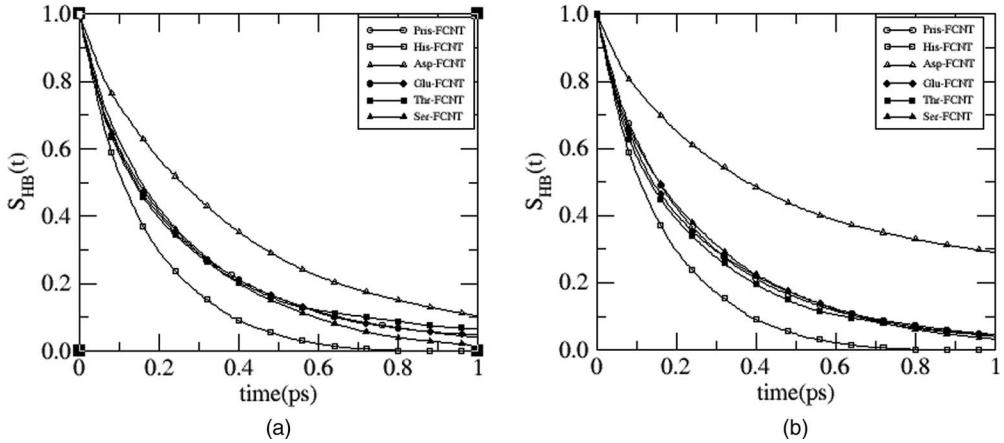

FIG. 13. Relaxation of the continuous hydrogen bond time correlation function (a) considering OW–OW hydrogen bonds between inner water molecules only and (b) considering X–OW hydrogen bonds along with OW–OW hydrogen bonds in pristine CNT (○), His-FCNT (□), Asp-FCNT (△), Glu-FCNT (●), Thr-FCNT (■), and Ser-FCNT (▲).

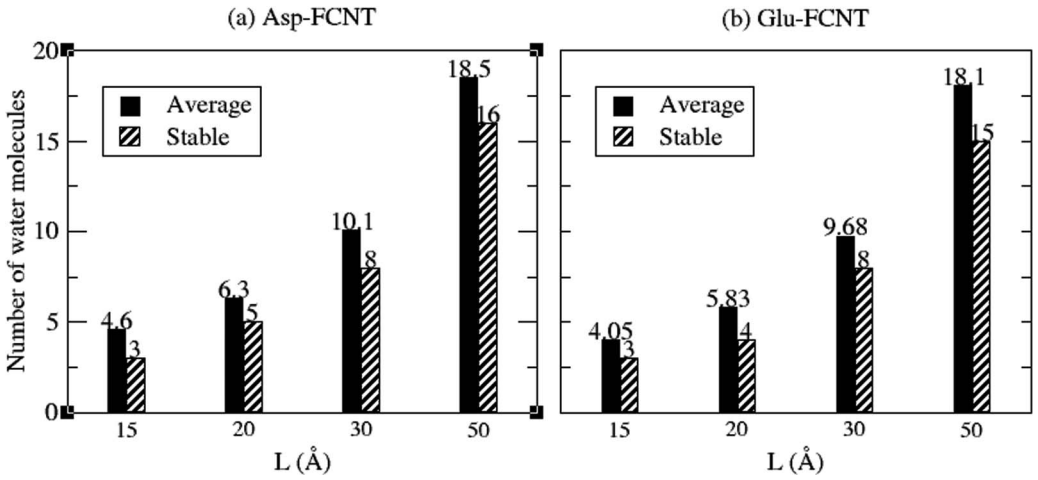

FIG. 15. Number of inner water molecules present inside (a) Asp- and (b) Glu-FCNTs of different lengths, L of the nanotube. The solid boxes represent the average number, $\bar{N}_{int}$ while the striped boxes correspond to the number of stable water molecules N_s, defined as those residing within the nanotube in more than 99% of the sampled structures.

F. Energetics and entropy of inner water molecules

We have compared the distribution of potential energy of inner water molecules (per mol) for different CNTs of length 15 Å to understand if energetic contributions favor the filling of these systems with water at room temperature. As shown in Fig. 17, similar to the pristine CNT, all the FCNTs (except His-FCNT) exhibit a favorable distribution of potential energy inside the core of the nanotube with Asp-FCNT exhibiting the largest stabilization. The pristine CNT and Glu-FCNT, on the other hand, are found to have nearly superimposable distribution. His-FCNT displays a sharp peak at zero potential energy corresponding to those configurations where no inner water molecules are present in the system.

We have also carried out a preliminary investigation of the entropy values for inner water molecules in our simulated systems using the 2PT method.[12,51,52] The total (translational plus rotational) entropy per water molecule inside pristine CNT is found to be 5.73 kcal/mole that agrees closely to the value obtained by Kumar *et al.*[12] (∼5.51 kcal/mole). In Asp- and Glu-FCNTs, total entropy per water molecule is

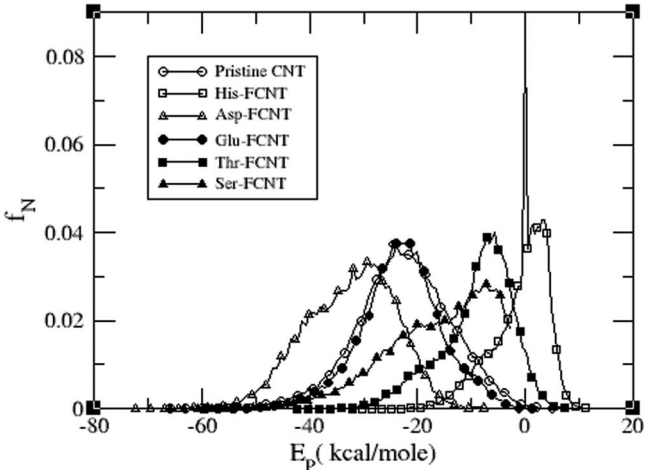

FIG. 17. Normalized distribution, f_N of intermolecular potential energy, E_p of inner water molecules inside pristine and functionalized CNTs.

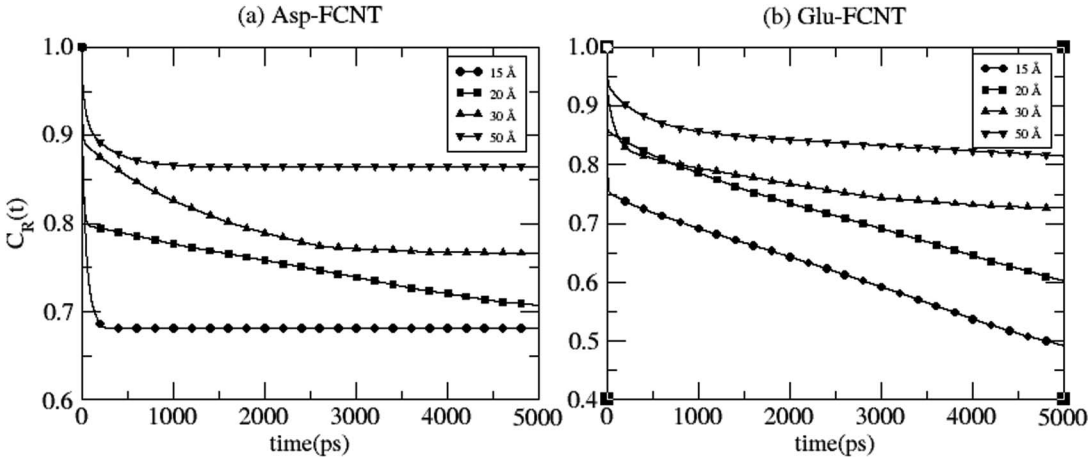

FIG. 16. Residential time correlation function of inner water molecules in (a) Asp- and (b) Glu-FCNT of lengths (a) 15 Å (●), (b) 20 Å (■), (c) 30 Å (▲), and (d) 50 Å (▼).

estimated to be 5.36 and 5.14 kcal/mole, respectively. These values fall short of that obtained for pristine CNT, but exceed that of bulk water (∼4.9 kcal/mole). Within the framework of 2PT method, inner water molecules in Asp- and Glu-FCNTs are found to have little translational entropy, but substantially large rotational entropy. The latter causes the entropy in these systems to be even greater than pristine CNT. This preliminary analysis agrees well with our observation of favorable retention of water molecules inside Asp- and Glu-FCNTs. However, as discussed earlier, accurate evaluation of the entropy of transfer of water from bulk to the interior of a CNT-based system may require a much more detailed investigation, especially in view of the recent reports by Waghe *et al.*[13]

IV. CONCLUSION

We have been able to demonstrate in this article that when put in water, endohedrally functionalized single-walled carbon nanotubes allow the spontaneous entry and retention of water molecules inside the core of the nanotube. Well ordered hydrogen bonded chains of water molecules are formed similar to those observed in the case of pristine CNTs. However, in the systems studied here, the extent of orientational ordering and lifetime of such water-mediated chains are found to depend crucially on the group suspended from the nanotube wall within the core. The −COOH groups of Asp- and Glu-FCNTs correspondingly allow the formation of longest water chains with larger residence times within the core. By comparing the results of Asp- and Glu-FCNTs, we have also been able to assess how the presence of a single additional $-CH_2$ group may affect the water retention capability of a single −COOH group in the given hydrophobic environment. The average number of inner water molecules is also found to be high in Ser-FCNTs. However, conformational fluctuations of the suspended sidechain are found to allow a much lower number of *stable* water molecules. Therefore, for the given standard choice of geometry ($L = 15.6$ Å and $\sigma = 8.2$ Å) of the FCNTs, taking $\bar{N}_{int}$, N_s, and $\langle \tau_R \rangle$ into account, the following order is predicted for their water retention capability: $Asp - FCNT > Glu - FCNT > Thr - FCNT$. The use of a longer nanotube is also found to result in a nearly linear increase in the number of water molecules being retained within the tube. It is also shown that the filling of the FCNTs (except for His-FCNT) with water at room temperature is expected to be favored by both energetic and entropic considerations.

The present work puts forward the need to have a close look at the seemingly improbable use of FCNTs as water storage devices. Even within the limited scope of the present studies, it is strongly indicated that bundles of long CNTs with appropriate endo- and exohedral funtionalizations may be able to retain layers of water within their individual cores as well as in the space intervening different tubes. However, it needs to be realized experimentally. In any case, this certainly merits as a new addition to novel applications of nanotube based systems including artificial enzymes.[53]

Our results may also be utilized in understanding the relative propensities of these amino acid sidechain analogues to control the structure and dynamics of neighboring water molecules in hydrophobic confinement. The presence of Asp-, Glu-, and Ser-like sidechains are found to have more impact on the equilibrium correlation between inner water molecules thereby leading to the formation of extended water chains. However, the dynamics of these chains vary depending on the nature and number of hydrogen bonding sites, X on the sidechain analogue. While Asp- and Glu-FCNTs turn out to be more suitable for retaining the largest number of inner water molecules, comparatively fast dynamical expulsion of inner water molecules is observed in Ser-FCNT. A comparison of the results for Asp/Glu- and Ser/Thr-like sidechains demonstrate how the presence of a $-CH_2$ or $-CH_3$ group can fine-tune the hydrophobic components of interaction between the suspended sidechain and inner water molecules. It is this aspect of our results that can be useful in fabricating model membranes and channels for better controlled transport of ions and solutions.

It may be noted that we have not focussed on issues such as ionization states of suspended groups. This will certainly be an important point to consider if one tries to map our results on to the biological systems where the amino acid sidechains are found to play an important role in managing the structure and dynamics of water molecules. Recent observations on the preparation of robust catalysts by incorporating suitable ionic moieties inside the CNT[54] lend further credential to the need for extending the present work where the effect of ionized groups suspended/restricted inside the hydrophobic core will be examined. Work is in progress in this direction.

ACKNOWLEDGMENTS

We sincerely thank Professor Sanjoy Bandyopadhyay for several helpful comments and discussions. This study was supported in part by a grant from Council for Scientific and Industrial Research (CSIR), India, and DST-FIST (SR/FST/CSII-011/2005), India.

[1] J. C. Rasaiah, S. Garde, and G. Hummer, Annu. Rev. Phys. Chem. **59**, 713 (2008).
[2] C. Song and B. Corry, J. Phys. Chem. B **113**, 7642 (2009).
[3] C. Peter and G. Hummer, Biophys. J. **89**, 2222 (2005).
[4] E. Mamontov, C. J. Burnham, S.-H. Chen, A. P. Moravsky, C.-K. Loong, N. R. de Souza, and A. I. Kolesnikov, J. Chem. Phys. **124**, 194703 (2006).
[5] A. I. Kolesnikov, J.-M. Zanotti, C.-K. Loong, P. Thiyagarajan, A. P. Moravsky, R. O. Loutfy, and C. J. Burnham, Phys. Rev. Lett. **93**, 035503 (2004).
[6] N. Naguib, H. Ye, Y. Gogotsi, A. G. Yazicioglu, C. M. Megaridis, and M. Yoshimura, Nano Lett. **4**, 2237 (2004).
[7] N. R. de Souza, A. Kolesnikov, C. Burnham, and C.-K. Loong, J. Phys.: Condens. Matter **18**, S2321 (2006).
[8] G. Hummer, J. C. Rasaiah, and J. P. Noworyta, Nature (London) **414**, 188 (2001).
[9] A. Alexiadis and S. Kassinos, Chem. Rev. **108**, 5014 (2008).
[10] B. Mukherjee, P. K. Maiti, C. Dasgupta, and A. K. Sood, J. Chem. Phys. **126**, 124704 (2007).
[11] S. Vaitheeswaran, J. C. Rasaiah, and G. Hummer, J. Chem. Phys. **121**, 7955 (2004).
[12] H. Kumar, B. Mukherjee, S.-T. Lin, C. Dasgupta, A. K. Sood, and P. K. Maiti, J. Chem. Phys. **134**, 124105 (2011).
[13] A. Waghe, J. C. Rasaiah, and G. Hummer, J. Chem. Phys. **137**, 044709 (2012).
[14] B. Mukherjee, P. K. Maiti, C. Dasgupta, and A. K. Sood, J. Phys. Chem. B **113**, 10322 (2009).
[15] I. Hanasaki and A. Nakatani, J. Chem. Phys. **124**, 174714 (2006).

[16]C. Dellago, M. M. Naor, and G. Hummer, Phys. Rev. Lett. **90**, 105902 (2003).
[17]A. Bankura and A. Chandra, J. Phys. Chem. B **116**, 9744 (2012).
[18]D. Pantarotto, J.-P. Briand, M. Prato, and A. Bianco, Chem. Commun. **2004**, 16.
[19]L. Lacerda, A. Bianco, M. Prato, and K. Kostarelos, Adv. Drug Delivery Rev. **58**, 1460 (2006).
[20]V. Georgakilas, K. Kordatos, M. Prato, D. M. Guldi, M. Holzinger, and A. Hirsch, J. Am. Chem. Soc. **124**, 760 (2002).
[21]J. L. Bahr, J. Yang, D. V. Kosynkin, M. J. Bronikowski, R. E. Smalley, and J. M. Tour, J. Am. Chem. Soc. **123**, 6536 (2001).
[22]D. Tasis, N. Tagmatarchis, A. Bianco, and M. Prato, Chem. Rev. **106**, 1105 (2006).
[23]J. E. Riggs, Z. Guo, D. L. Carroll, and Y.-P. Sun, J. Am. Chem. Soc. **122**, 5879 (2000).
[24]K. C. Park, T. Hayashi, H. Tomiyasu, M. Endo, and M. S. Dresselhaus, J. Mater. Chem. **15**, 407 (2005).
[25]S. Joseph, R. J. Mashl, E. Jakobsson, and N. R. Aluru, Nano Lett. **3**, 1399 (2003).
[26]J. Zheng, E. M. Lennon, H.-K. Tsao, Y.-J. Sheng, and S. Jiang, J. Chem. Phys. **122**, 214702 (2005).
[27]X. Gong, J. Li, K. Xu, J. Wang, and H. Yang, J. Am. Chem. Soc. **132**, 1873 (2010).
[28]L. Janosl and M. Ceccarelli, PLOS ONE **8**, e59897 (2013).
[29]M. Wikstrm, Curr. Opin. Struct. Biol. **8**, 480 (1998).
[30]T. G. Abi, A. Anand, and S. Taraphder, J. Phys. Chem. B **113**, 9570 (2009).
[31]T. Abi and S. Taraphder, Chem. Phys. **405**, 107 (2012).
[32]D. Case, T. Darden, T. Cheatham III, C. Simmerling, J. Wang, R. Duke, R. Luo, R. Walker, W. Zhang, K. Merz *et al.*, AMBER12 (University of California, San Francisco, 2012).
[33]A. W. Gtz, M. J. Williamson, D. Xu, D. Poole, S. Le Grand, and R. C. Walker, J. Chem. Theory Comput. **8**, 1542 (2012).
[34]B. Delley, Comput. Mater. Sci. **17**, 122 (2000).
[35]J. Tirado-Rives and W. L. Jorgensen, J. Chem. Theory Comput. **4**, 297 (2008).
[36]W. L. Jorgensen, J. Chandrasekhar, J. D. Madura, R. W. Impey, and M. L. Klein, J. Chem. Phys. **79**, 926 (1983).
[37]T. Darden, D. York, and L. Pedersen, J. Chem. Phys. **98**, 10089 (1993).
[38]A. Luzar and D. Chandler, Nature (London) **379**, 55 (1996).
[39]B. Bagchi, Chem. Rev. **105**, 3197 (2005).
[40]M. Jana and S. Bandyopadhyay, J. Phys. Chem. B **115**, 6347 (2011).
[41]S. Pal and S. Bandyopadhyay, Langmuir **29**, 1162 (2013).
[42]P. L. Chau and A. J. Hardwick, Mol. Phys. **93**, 511 (1998).
[43]J. R. Errington and P. G. Debenedetti, Nature (London) **409**, 318 (2001).
[44]B. S. Jabes, M. Agarwal, and C. Chakravarty, J. Chem. Phys. **132**, 234507 (2010).
[45]N. Bhattacharjee and P. Biswas, Biophys. Chem. **158**, 73 (2011).
[46]B. Song and V. Molinero, J. Chem. Phys. **139**, 054511 (2013).
[47]D. Bandyopadhyay, S. Mohan, S. K. Ghosh, and N. Choudhury, J. Phys. Chem. B **117**, 8831 (2013).
[48]D. Nayar and C. Chakravarty, Phys. Chem. Chem. Phys. **15**, 14162 (2013).
[49]M. Jana and S. Bandyopadhyay, J. Phys. Chem. B **117**, 9280 (2013).
[50]T. D. Kuehne and R. Z. Khaliullin, J. Am. Chem. Soc. **136**, 3395 (2014).
[51]S.-T. Lin, M. Blanco, and W. A. Goddard, J. Chem. Phys. **119**, 11792 (2003).
[52]S.-T. Lin, P. K. Maiti, and W. A. Goddard, J. Phys. Chem. B **114**, 8191 (2010).
[53]Y. Lin, J. Ren, and X. Qu, Acc. Chem. Res. **47**, 1097 (2014).
[54]R. S. Dey, R. K. Bera, and C. R. Raj, Anal. Bioanal. Chem. **405**, 3431 (2013).